HYBRID D^3 SIGMA-DELTA STAP ALGORITHM IN NON-HOMOGENEOUS CLUTTER

Eunjung Yang*, Raviraj Adve†, Joohwan Chun*, and Jonghoon Chun††

*School of Electrical Engineering and Computer Science, KAIST, 373-1 Guseong-dong, Youseong-gu, Daejeon 305-701, Korea ejyang@sclab.kaist.ac.kr , chun@ee.kaist.ac.kr

†Department of Electrical and Computer Engineering, University of Toronto,10 King's College Rd. Toronto, Ontario M5S 3G4, Canada rsadve@comm.utoronto.ca

††SAMSUNG THALES CO. Ltd, Chang-Li 304, Namsa-myun, Cheoin-gu, Yongin-city, Gyeonggi-do 446-885, Korea jonghoon.chun@samsung.com

Keywords: D^3 algorithm, Sigma-Delta STAP, Two-stage hybrid algorithm, non-homogeneous clutter environment

Abstract

The need to deal with non-homogeneous clutter has driven much of the recent research in space-time adaptive processing (STAP). This paper presents an extension of the low-complexity, sigma-delta (ΣΔ) algorithm incorporating the direct data domain (D^3) processing. The new algorithm is practical and improves target detection in non-homogeneous clutter environments. The algorithm employs a hybrid approach, combining D^3 processing with the more traditional statistical approach, thereby obtaining advantages of both. In this paper, first, a modified D^3 algorithm, which maximizes signal-to-interference-plus-noise ratio, is presented. Then this D^3 algorithm is used as an adaptive transformer to create sum (Σ) and difference (Δ) beams. The residual interference after the D^3 processing is further cancelled by ΣΔ STAP. The proposed hybrid algorithm using D^3-ΣΔ STAP is tested in non-homogeneous clutter modelled using spherically invariant random variables (SIRV) and artificially injected discrete interferers. Performance of the proposed methods is compared with those of traditional statistical approaches, illustrating significant benefits of hybrid processing in non-homogeneous scenarios.

1 Introduction

In an airborne radar system, ground clutter is the most severe interference and must be suppressed to detect relatively weak moving targets. The ground clutter's correlated characteristic in the angle-Doppler domain requires traditional array signal processing be extended to space time adaptive processing (STAP) [4]. Consider the operation of an airborne phased array radar with N antennas processing M pulses within each coherent processing interval (CPI). The STAP algorithm assigns the optimal complex weight to each of the NM degrees-of-freedom (DOF) within one range cell at a time. The optimal weight vector is generally found in the minimum mean squared error (MMSE) sense assuming Gaussian interference.

It is now well accepted that several fundamental issues make it impossible to implement the theoretically optimal and straightforward algorithm in practical radar systems. An obvious problem with fully adaptive processing is high computation load, $O[(MN)^3]$ per range cell; however, more fundamental limitation is the one with limited available training samples. The interference covariance matrix is unknown *a priori* and must be estimated in real-time via training samples, usually obtained from range cells other than the range cell under test. Clearly, for the training to be effective, the interference statistics of secondary cell should match that of the test cell, i.e., the training data should be target free and homogeneous.

The problem with training arises because the Reed-Mallet-Brennan rule [3] states that a reasonably accurate estimate of the interference covariance matrix requires that the number of training samples be at least twice the DOF, i.e., estimating the interference covariance matrix requires at least $2NM$ training samples, which are generally not available in practice. Furthermore, training samples should be statistically homogeneous, i.e., the ground clutter (and hence the ground itself) must be homogeneous over the entire training sample set. Typically most environments in which STAP operates are non-homogeneous, for example, due to terrain variations. The performance of traditional statistical algorithms using covariance matrices to determine the adaptive weights deems to be degraded in non-homogeneous environments. The importance and impact of non-homogeneous environments has been discussed in some detail in, for example, [12][19][20] and references therein.

Several recent works have solved the problems with computation load and required training samples via reduced DOF schemes [2, 8, 9, 10]. Of particular interests in our work are transform domain approaches wherein adaptive processing takes place after transformation to the angle-Doppler space [2, 9, 10]. In the joint domain localized (JDL) algorithm, adaptive processing occurs within a localized processing region (LPR) after transformation to angle-Doppler space. The LPR comprises η_a angles and η_d Doppler bins (where η_a and η_d are generally much smaller than N and M, respectively). In these approaches the angle-Doppler weights are obtained by $\tilde{\mathbf{w}} = \tilde{\mathbf{R}}^{-1}\tilde{\mathbf{s}}$, based on the estimated angle-Doppler interference covariance matrix $\tilde{\mathbf{R}}$ and the angle-Doppler steering vector $\tilde{\mathbf{s}}$. The equivalent space-time weight vectors are then given by $\mathbf{w} = \mathbf{T}\tilde{\mathbf{w}}$, where $\mathbf{T}$ is the angle-Doppler transformation matrix. On the other hand, in ΣΔ processing of [8], sum (Σ) and difference (Δ) beams are formed and then adaptively combined. In either case, the overall DOF used is significantly reduced with attendant reduction in required computation load and training samples.

However, despite the required number of training samples are reduced, the need for homogeneity of training samples remains unresolved. The variation of interference within secondary sample support leads to an inaccurate estimate of the interference statistics in the cell under test. To overcome the difficulties, a non-homogeneity detector (NHD) is used so as to identify non-homogeneous range cells [21, 22]. Once identified, non-homogeneous range cells can be removed from the secondary sample set used to estimate interference statistics.

Another cause of non-homogeneous environments is discrete interferers, such as coherent repeat jammers or other local interference sources, which exist within the cell under test i.e., the primary range cell. Since the secondary samples have no information about these local interferers, traditional statistical algorithms are not able to suppress them. In this regard an interesting advance has been the development of the direct data domain (D^3) algorithm that can handle discrete interferers in the primary range cell [13]. The approach is to adaptively minimize the interference power while maintaining array gain to the direction of the signal. Not having to estimate covariance matrices eliminates the sample support problem and hence the D^3 algorithm is particularly effective against non-homogeneous interference. However, ignorance of correlation between range cells lets D^3 approaches not as effective against correlated interference.

In [11], a two-stage hybrid algorithm was proposed, combining the D^3 algorithm with traditional JDL processing to achieve the benefits of both. This hybrid approach basically employs the JDL framework and uses the D^3 weight as a first-stage filter to suppress discrete interferers present in the range cell under test. This first stage serves as an adaptive transformer from the space-time to angle-Doppler domain replacing the steering vector based non-adaptive transformer used in the original JDL algorithm. The hybrid algorithm played a crucial role in the use of knowledge based STAP (KB-STAP) wherein the adaptive algorithm is chosen to best match the interference scenario at hand [12].

This paper addresses two issues raised by the two-stage hybrid algorithm as currently available in [11]. In [11], the first D^3 stage is based on the maximization of the difference between terms related to the power of a target and interference. Maximizing this difference leads to unstable solutions requiring a good choice of the emphasis parameter weighing one term versus the other via trial and error. However, it is difficult to select an appropriate

parameter because the performance of the algorithm is highly sensitive to a small variation of the parameter value. Here the D^3 algorithm is modified to remove the emphasis parameter while maintaining the original framework. The new algorithm is reformulated to maximize the signal to interference plus noise ratio (SINR) employing the forward smoothing technique [26] as well to make the method more reliable. Furthermore we adopt a projection-based method [23, 24] for the D^3 algorithm to alleviate signal cancellation under calibration error.

Another issue of the hybrid algorithm in [11] is that of computation load. When η_a angle bins and η_d Doppler bins in the localized processing region (LPR) are chosen for the second stage, the D^3 algorithm must be executed $\eta_a \eta_d$ times at each range cell while the original JDL uses predetermined non adaptive steering vectors. Therefore, with the hybrid algorithm the reduction of the DOF has more impact on the total computation load compared to the non-hybrid algorithm. In [12], this problem is addressed in a knowledge based approach by using a JDL-based non-homogeneity detector (NHD) and applying the hybrid algorithm only for those range cells declared non-homogeneous.

While the JDL algorithm reduces the degrees of freedom from *NM* to $\eta_a \eta_d$ which is usually a much smaller number, an even more efficient algorithm is the ΣΔ algorithm [8]. The ΣΔ algorithm was first developed in the context of adding STAP capability to systems based on analog sum and difference beams. However, this approach can also be employed for systems using digital beamforming. One of main contributions of this paper is the ΣΔ based hybrid algorithm, where the ΣΔ strategy is applied to Doppler as well as angle domain. A crucial step is a new development of a D^3 version of the difference or Δ beam. The overall approach combines the benefits of D^3 and statistical processing while being both stable and efficient.

This paper is organized as follows. In Section 2, a modified D^3 algorithm is introduced. An extension to the ΣΔ based hybrid algorithm is given in Section 3, and combined-STAP using two stage hybrid algorithms and NHD is summarized in Section 4. Numerical results illustrating the efficacy of the proposed ΣΔ based hybrid approaches are presented in Section 5. Finally, Section 6 presents some conclusions and suggestions for future directions.

2 Direct data domain (D^3) algorithm

In [13] an algorithm that obtains adaptive weights is developed, in the least squares sense, for signals impinging from a fixed look-direction. This method minimizes the error between the received voltages (signal plus noise) and a signal from the look angle. This approach does not employ data from outside the radar range cell being evaluated, i.e., this method does not require secondary data. This makes the algorithm an attractive alternative to traditional statistical processing in the presence of non-homogeneous clutter. The original algorithm in [13] focuses on one-dimensional spatial adaptivity. This work has later been extended to two-dimensional space-time processing in [11] where the authors maximize the difference between the signal and interference power after adaptive processing. The most serious drawback is that these two terms are balanced via the so-called emphasis parameter that is picked in either an ad hoc manner or via exhaustive search. Since this algorithm forms a basis of our D^3 processing, we briefly describe it below before proposing the new algorithm.

Consider a linear array with *N* antennas uniformly spaced with the half wavelength separation, where *M* pulses are transmitted with a PRF of f_r within a CPI. For a target direction of ϕ_t, with the angle referred to broadside, the signal advances from one element to the next by the phase factor $z_s=\exp(j\pi\sin(\phi_t))$. Associated with this direction the spatial steering vector is $\mathbf{a}(\phi_t) = [\,1, z_s, z_s^2, \ldots, z_s^{N-1}]^T$, where $(\cdot)^T$ denotes transposition. Similarly, for a target Doppler frequency of f_t, the phase of the target signal advances from one pulse to the next by the factor of $z_t=\exp(j2\pi f_t/f_r)$ resulting a temporal steering vector of $\mathbf{b}(f_t) = [\,1, z_t, z_t^2, \ldots, z_t^{M-1}]^T$.

The scheme in [11] computes spatial and temporal weight vectors independently.

For the spatial D^3 weight vector, defining x_{nm} as the signal received at the n-th element and the m-th pulse within the range cell under test, the term, $x_{nm} - z_s^{-1}x_{(n+1)m}$ is free of target and contains interference only. The D^3 algorithm minimizes the interference power while maintaining a finite gain in the look direction. To best present the D^3 algorithm, the signal from the N antennas due to M pulses in a CPI is written as an $N\times M$ matrix $\mathbf{X}$ whose m-th column corresponds to the N returns from the m-th pulse. The received signal can be represented as a sum of the target signal and interference terms

$$\mathbf{X} = \alpha_s \mathbf{S}\left(\phi_t, f_t\right) + \mathbf{C} + \mathbf{J} + \mathbf{N}, \tag{1}$$

where α_s is the target amplitude and $\mathbf{S}(\phi_t, f_t) = \mathbf{a}(\phi_t)\ \mathbf{b}(f_t)^{\mathrm{T}}$ is the space-time steering matrix corresponding to the look direction of ϕ_t and look Doppler of f_t . The matrices $\mathbf{C}$, $\mathbf{J}$ and $\mathbf{N}$ represent clutter, jammer and noise signals, respectively.

Define the $(N\text{-}1) \times M$ matrix $\mathbf{A}$ to be

$$\mathbf{A} = \begin{bmatrix} \mathbf{X}_{00} - z_s^{-1}\mathbf{X}_{10} & \mathbf{X}_{01} - z_s^{-1}\mathbf{X}_{11} & \cdots & \mathbf{X}_{0(M-1)} - z_s^{-1}\mathbf{X}_{1(M-1)} \\ \mathbf{X}_{10} - z_s^{-1}\mathbf{X}_{20} & \mathbf{X}_{11} - z_s^{-1}\mathbf{X}_{21} & \cdots & \mathbf{X}_{1(M-1)} - z_s^{-1}\mathbf{X}_{2(M-1)} \\ \vdots & \vdots & \vdots & \vdots \\ \mathbf{X}_{(N-2)0} - z_s^{-1}\mathbf{X}_{(N-1)0} & \mathbf{X}_{(N-2)1} - z_s^{-1}\mathbf{X}_{(N-1)1} & \cdots & \mathbf{X}_{(N-2)(M-1)} - z_s^{-1}\mathbf{X}_{(N-1)(M-1)} \end{bmatrix}, \tag{2}$$

where $\mathbf{X}_{i,j}$ denotes the (i, j) element of $\mathbf{X}$, and define the length $N\text{-}1$ spatial steering vector $\mathbf{a}_{(0:N\text{-}2)}$ of the look direction ϕ_t and length $N\text{-}1$ spatial weight vector $\mathbf{w}_s$. Both vectors are of length $N\text{-}1$ due to the one DOF lost to the subtraction operation. The original D^3 algorithm of [11] maximizes the difference between output power from target and the interference:

$$\max_{\|\mathbf{w}_s\|_2=1}[R_{\mathbf{w}_s}] = \max_{\|\mathbf{w}_s\|_2=1}[\ T_{\mathbf{w}_s} - \kappa^2 I_{\mathbf{w}_s}] = \max_{\|\mathbf{w}_s\|_2=1}\ \mathbf{w}_s^H[\mathbf{a}_{(0:N-2)}\mathbf{a}_{(0:N-2)}^H\ \ -\kappa^2\ \ \mathbf{A}\mathbf{A}^H]\mathbf{w}_s$$

where

$$\begin{aligned} T_{\mathbf{w}_s} &= \left|\mathbf{w}_s^H\mathbf{a}_{(0:N-2)}\right|^2 = \mathbf{w}_s^H\mathbf{a}_{(0:N-2)}\mathbf{a}_{(0:N-2)}^H\mathbf{w}_s\,, \\ I_{\mathbf{w}_s} &= \left\|\mathbf{w}_s^H\mathbf{A}\right\|^2 = \mathbf{w}_s^H\mathbf{A}\mathbf{A}^H\mathbf{w}_s\,, \text{ and} \\ R_{\mathbf{w}_s} &= T_{\mathbf{w}_s} - \kappa^2 I_{\mathbf{w}_s} = \mathbf{w}_s^H\mathbf{a}_{(0:N-2)}\mathbf{a}_{(0:N-2)}^H\mathbf{w}_s\ \ -\kappa^2\ \ \mathbf{w}_s^H\mathbf{A}\mathbf{A}^H\mathbf{w}_s. \end{aligned} \tag{3}$$

Here, $(\cdot)^H$ denotes conjugate transposition. The term κ in the definition of $R_{\mathbf{w}_s}$ represents a parameter to emphasize the power gain on either the target or interference. The D^3 algorithm finds the spatial weight $\mathbf{w}_s$ that maximizes $R_{\mathbf{w}_s}$ with the constraint of $\|\mathbf{w}_s\|_2 = 1$ which guarantees a non-zero solution. Using the method of Lagrange multipliers, it can be shown that the desired spatial weight vector is the eigenvector associated with the maximum eigenvalue of the $(N\text{-}1)\times(N\text{-}1)$ matrix $[\mathbf{a}_{(0:N-2)}\mathbf{a}_{(0:N-2)}^H - \kappa^2\ \ \mathbf{A}\mathbf{A}^H]$.

A significant drawback with the above approach is that the performance of the D^3 method is sensitive to the choice of the emphasis parameter κ. In this paper we make a fairly simple modification of the D^3 algorithm, based on the well-known concept of maximizing the signal-to-interference pulse noise ratio (SINR) [1]. When $I_{\mathbf{w}_s}$ in equation (3) is redefined as $I_{\mathbf{w}_s} = \mathbf{w}_s^H\left(\frac{1}{M}\mathbf{A}\mathbf{A}^H\right)\mathbf{w}_s$, this serves as a proxy for the residual interference

power after the data are filtered by the weight $\mathbf{w}_s$. Here, $\hat{\mathbf{R}} = (\mathbf{A}\mathbf{A}^H)/M$ acts as a sample spatial covariance matrix (where samples are taken over different pulses) in the cell under test. The target signal power $T_{\mathbf{w}_s}$ is also redefined as in Eqn. (4) using the target signal amplitude α_s:

$$T_{\mathbf{w}_s} = \left\| \mathbf{w}_s^H (\alpha_s \mathbf{a}_{(0:N-2)}) \right\|^2 = |\alpha_s|^2 \, \mathbf{w}_s^H \mathbf{a}_{(0:N-2)} \mathbf{a}_{(0:N-2)}^H \mathbf{w}_s . \tag{4}$$

Using the two terms defined above, the effective SINR is

$$\text{SINR} = \frac{T_{\mathbf{w}_s}}{I_{\mathbf{w}_s}} = \frac{|\alpha_s|^2 \, \mathbf{w}_s^H \mathbf{a}_{(0:N-2)} \mathbf{a}_{(0:N-2)}{}^H \mathbf{w}_s}{\mathbf{w}_s^H \left(\frac{1}{M} \mathbf{A}^T \mathbf{A}^* \right) \mathbf{w}_s} = \frac{|\alpha_s|^2 \, \mathbf{w}_s^H \mathbf{a}_{(0:N-2)} \mathbf{a}_{(0:N-2)}{}^H \mathbf{w}_s}{\mathbf{w}_s^H \hat{\mathbf{R}} \mathbf{w}_s} . \tag{5}$$

Now the modified D^3 algorithm maximizes the SINR in (5), resulting the weight vector $\mathbf{w}_s = (\hat{\mathbf{R}})^{-1} \mathbf{a}_{(0:N-2)}$ assuming $\hat{\mathbf{R}}$ is non-singular. As we can see in (2), the matrix $\mathbf{A}$ contains only interference terms, therefore in most cases $\hat{\mathbf{R}}$ can be assumed to be non-singular. If this matrix is singular then the weight vector may be obtained using the pseudo-inverse or diagonal loading [1, 18]. The proposed algorithm using the SINR maximizing strategy is, therefore, simple and has no need for an emphasis parameter κ. Once we obtain the length N-1 spatial weight vector $\mathbf{w}_s$, we set $\mathbf{w}_s = [\mathbf{w}_s^T \;\; 0]^T$ appending a zero to restore the loss of the single DOF.

In the SINR based D^3 algorithm, the matrix $\hat{\mathbf{R}}$ may be viewed as an interference covariance matrix estimated by M snapshots which may not be enough for adequate estimation. To make the algorithm even more stable, the forward smoothing technique of [26] is applied. This technique uses a sliding window with the size of $N_s \times 1$ to slide over the matrix $\mathbf{A}$, where $N_s (\le N-1)$ is the number of spatial DOF. Then, we can get $L = (N - N_s)M$ subvectors which may be enough for adequate covariance estimation, at the cost of DOF losses. Let

$$\begin{aligned} &\mathbf{z}_{i,k} = \mathbf{A}[i : i + N_s - 1, k], \quad i = 1, \cdots, N - N_s \;\; , \;\; k = 1, \cdots, M \\ &\overline{\mathbf{a}}_l = \mathbf{z}_{i,k}, \quad l = (k-1)(N - N_s) + i \\ &\overline{\mathbf{A}} = [\overline{\mathbf{a}}_1, \; \overline{\mathbf{a}}_2, \; \cdots, \overline{\mathbf{a}}_L]. \end{aligned} \tag{6}$$

Replacing $\hat{\mathbf{R}} = (\mathbf{A}\mathbf{A}^H)/M$ with $\tilde{\mathbf{R}} = (\overline{\mathbf{A}}\overline{\mathbf{A}}^H)/L$, and $\mathbf{a}_{(0:N-2)}$ with $\mathbf{a}_{(0:N_s-1)}$ in the equation (5), the spatial weight vector is obtained as $\mathbf{w}_s = \tilde{\mathbf{R}}^{-1} \mathbf{a}_{(0:N_s-1)}$ with appropriate zeros appended. In our work, the DOF reduction is three, resulting $N_s = N - 1 - 3$ to get $L=4M$ available snapshots. Hence, 4 zeros (one is for the DOF lost to the subtraction operation in $\mathbf{A}$, the others are caused by additional DOF reduction to increase number of snapshots) should be appended at appropriate positions.

The temporal weight $\mathbf{w}_t$ is determined in a similar manner using the $(M-1)\times N$ matrix $\mathbf{B}$ as defined below

$$\mathbf{B} = \begin{bmatrix} \mathbf{X}_{00} - z_t^{-1}\mathbf{X}_{01} & \mathbf{X}_{10} - z_t^{-1}\mathbf{X}_{11} & \cdots & \mathbf{X}_{(N-1)0} - z_t^{-1}\mathbf{X}_{(N-1)1} \\ \mathbf{X}_{01} - z_t^{-1}\mathbf{X}_{02} & \mathbf{X}_{11} - z_t^{-1}\mathbf{X}_{12} & \cdots & \mathbf{X}_{(N-1)1} - z_t^{-1}\mathbf{X}_{(N-1)2} \\ \vdots & \vdots & \vdots & \vdots \\ \mathbf{X}_{0(M-2)} - z_t^{-1}\mathbf{X}_{0(M-1)} & \mathbf{X}_{1(M-2)} - z_t^{-1}\mathbf{X}_{1(M-1)} & \cdots & \mathbf{X}_{(N-1)(M-2)} - z_t^{-1}\mathbf{X}_{(N-1)(M-1)} \end{bmatrix}, \tag{7}$$

the temporal steering vector of the look Doppler f_t, $\mathbf{b}(f_t)$, and the number of temporal DOF $N_t (\le M-1)$.

Once we obtain the length N spatial weight vector $\mathbf{w}_s$ and the length M temporal weight vector $\mathbf{w}_t$, the length-MN space time adaptive weight vector is given by $\mathbf{w}(\phi_t, f_t) = \mathbf{w}_t \otimes \mathbf{w}_s$, where $\otimes$ denotes the Kronecker tensor product.

The development so far has ignored array effects such as mutual coupling, channel mismatch or array imperfections. In a practical setting, these must be eliminated using a calibration or compensation technique [11, 17, 21, 23, 24]. In this paper, we shall show that the simple projection-based compensation method in [24] gives good performance for the D^3 algorithm under calibration error.

The $N_s \times N_s$ spatial covariance matrix can be decomposed into its eigenvalues and outer products of corresponding eigenvectors, the leading K $(K \le N_s)$ eigenvectors span the signal subspace and the remaining eigenvectors associated with small eigenvalues span the noise subspace, where K is the effective rank of the covariance matrix:

$$\tilde{\mathbf{R}} = \sum_{i=1}^{K} \lambda_i \mathbf{e}_i \mathbf{e}_i^H + \sum_{j=K+1}^{N_s} \lambda_j \mathbf{e}_j \mathbf{e}_j^H . \tag{8}$$

In the D^3 case the signal subspace is defined by the strong mainlobe clutter plus jammer signals, while the noise subspace is defined by negligible sidelobe clutter.

The spatial weight, $\mathbf{w}_s$, that optimizes the output SINR may be written as

$$\mathbf{w}_s = \tilde{\mathbf{R}}^{-1} \mathbf{a}_{(0:N_s-1)} = \sum_{i=1}^{K} \frac{1}{\lambda_i} \mathbf{e}_i (\mathbf{e}_i^H \mathbf{a}_{(0:N_s-1)}) + \sum_{j=K+1}^{N_s} \frac{1}{\lambda_j} \mathbf{e}_j (\mathbf{e}_j^H \mathbf{a}_{(0:N_s-1)}), \tag{9}$$

where $\mathbf{e}_i^H \mathbf{a}_{(0:N_s-1)}$ is a complex scalar p_i that represents the projection of the steering vector onto the signal subspace. Similarly, $\mathbf{e}_j^H \mathbf{a}_{(0:N_s-1)}$ is a complex scalar p_j that represents the projection of the steering vector onto the noise subspace. We note that the error-free exact steering vector $\mathbf{a}_{(0:N_s-1)}$ must lie on the signal subspace of $\tilde{\mathbf{R}}$, resulting $p_j = \mathbf{e}_j^H \mathbf{a}_{(0:N_s-1)} = 0$. However, if the steering vector has errors, p_j is nonzero and what the projection method does to reduce the effect of the steering vector error is to force $p_j = 0$.

$$\mathbf{w}_s = \sum_{i=1}^{K} \frac{1}{\lambda_i} \mathbf{e}_i (\mathbf{e}_i^H \mathbf{a}_{(0:Ns-1)}) . \tag{10}$$

Here a good choice of K could be found using for example the minimum description length (MDL) or Akaike information criterion (AIC) method [27].

Since the D^3 processing scheme uses samples from the primary range cell, it is possible to suppress a discrete interferer in the cell under test. Similarly, removing the requirement for secondary sample support makes it an attractive approach in a severely non-homogeneous environment. However, by ignoring correlation across range cells, the D^3 scheme is inherently unable to suppress correlated interference (such as distributed clutter and barrage noise jamming) [11]. This motivates the search for a hybrid approach that combines the benefits of both D^3 and statistical processing. This framework was first suggested in [11] wherein the drawbacks of D^3 processing were first documented.

3 Two-stage hybrid algorithm

In this section we present a hybrid algorithm based on the new D^3 approach of the section 2 and the ΣΔ statistical algorithm of [8]. We begin by briefly reviewing the original two-stage hybrid algorithm proposed in [11] combining the D^3 algorithm with JDL processing. The combination and sequencing of the two presented here is made possible because the JDL and ΣΔ STAP, beamspace algorithms, process data *after transformation to the angle-Doppler domain*

To describe the two-stage hybrid algorithm it is helpful to consider the general framework of JDL-STAP. The JDL algorithm begins with a non-adaptive transform of the samples from a space-time domain to a localized processing region (LPR) in the angle-Doppler domain. This is followed by a statistical detection algorithm

within the LPR in the angle-Doppler space. The main difference between JDL and the two-stage hybrid algorithm in [11] is the data transformation process. In the JDL algorithm, a domain transformation is achieved by an inner product with the steering vectors associated with the angle-Doppler points within the LPR. The hybrid algorithm of [11], on the other hand, uses an adaptive transformation based on the D^3 processing weights, replacing non-adaptive steering vectors. The key principle is that any adaptive process forms an estimate of the signal at the look angle/Doppler (comparing to a threshold for target detection is part of post-processing). As shown in Figure 1, the first stage of the hybrid algorithm uses D^3 weights to suppress discrete interferers in the cell under test and to transform the data domain simultaneously.

In both the JDL algorithm of [2] and the hybrid algorithm of [11], the transformation to the angle-Doppler domain is represented as multiplication of the space-time samples with a transformation matrix. For example, the transformation matrix of the JDL based hybrid algorithm for three angles (ϕ_{-1} ,ϕ_0 ,ϕ_1 ; $\eta_a = 3$) and three Doppler bins (f_{-1} ,f_0 ,f_1 ; $\eta_d = 3$) in the LPR is given by the $NM\times 9$ matrix

$$\mathbf{T} = [\mathbf{w}(\phi_{-1}, f_{-1}), \mathbf{w}(\phi_{-1} f_0), \mathbf{w}(\phi_{-1} f_1), \mathbf{w}(\phi_0, f_{-1}), \mathbf{w}(\phi_0 f_0), \mathbf{w}(\phi_0 f_1), \mathbf{w}(\phi_1, f_{-1}), \mathbf{w}(\phi_1 f_0), \mathbf{w}(\phi_1 f_1)], \qquad (11)$$

where $\mathbf{w}(\phi, f)$ is the D^3 weight for the look angle ϕ and look doppler f.

Once we get the transformation matrix **T**, it is used to transform the primary and secondary data to the angle-Doppler space. Furthermore, the target steering vector **s** is also transformed to the angle-Doppler domain using the same transformation matrix. Unfortunately, unlike the original JDL algorithm, the transformation matrix of the hybrid algorithm changes from a range cell to another. This is the major drawback of the hybrid algorithm which induces high computation load. To obtain a transformation matrix **T** for one range cell**,** $\eta_a \eta_d$ D^3-weight computations are needed (the new D^3-weight computation has at most $\mathbf{O}[((N-1)(N-1))^3]$+$\mathbf{O}[((M-1)(M-1))^3] = \mathbf{O}[((M-1)(M-1))^3]$ complexity, where $M \geq N$), while, in JDL, a predetermined transformation matrix is used for every test cell. The computation load associated with the hybrid algorithm is, therefore, significantly higher; by the order of ($L\times\eta_a\eta_d\times\mathbf{O}(((M-1)(M-1))^3) \times\mathbf{O}((\eta_a\eta_d)^3)$) compared to the JDL algorithm of $L\times\mathbf{O}((\eta_a\eta_d)^3)$, where L is the number of range cells to be tested. Reducing the DOF, therefore, has a great impact on the total computation load, setting the stage for an important contribution of a ΣΔ based hybrid algorithm in this paper.

3.1 ΣΔ-DDL based hybrid algorithm

We extend the hybrid concept to the ΣΔ algorithm of [8] wherein the adaptive processing focuses on just two spatial DOF (η_a=2), the sum (Σ) and difference (Δ) channels. In the ΣΔ-DDL STAP, DDL (Doppler domain localized) processing in the temporal domain and ΣΔ processing in the spatial domain are used as illustrated in Figure 2. In the ΣΔ-DDL based hybrid algorithm, we use the D^3 processing for both the cancellation of discrete interferers and the data transformation to the angle-doppler domain, followed by the traditional detection algorithm of ΣΔ-DDL STAP. In developing our algorithm, we exploit the fact that the space-time weight vector in the D^3 processing (as mentioned in Section 2) is computed by a Kronecker product of individual spatial and temporal weights. This makes it possible to separate spatial and temporal domain transformation for hybrid schemes.

To get Σ and Δ transformation matrix in terms of D^3 weights, some modifications are needed in the first stage rather than forming the sum and difference beams as products of steering vectors and appropriate tapers [8]. Note that the sum and difference beams can also be obtained based on two auxiliary look directions:

$$\mathbf{s}_s(\phi_t) = \{\mathbf{a}(\phi_L) + \mathbf{a}(\phi_R)\} \quad , \quad \mathbf{d}_s(\phi_t) = \{\mathbf{a}(\phi_L) - \mathbf{a}(\phi_R)\}\,, \qquad (12)$$

where $\phi_L = \phi_t - \phi_{del}$, $\phi_R = \phi_t + \phi_{del}$ with the look angle ϕ_t and angle interval ϕ_{del} ,and $\mathbf{a}(\phi)$ is the spatial steering vector for direction ϕ. The technique is extended to the ΣΔ-DDL based hybrid algorithm proposed here. Let spa-

tial D^3 weight vectors corresponding to ϕ_L and ϕ_R be $\mathbf{w}_s(\phi_L)$ and $\mathbf{w}_s(\phi_R)$ respectively, and define the corresponding sum and difference weight vectors as

$$\mathbf{w}_{s-\Sigma} = \mathbf{w}_s(\phi_L) + \mathbf{w}_s(\phi_R)\ ,\ \mathbf{w}_{s-\Delta} = \mathbf{w}_s(\phi_L) - \mathbf{w}_s(\phi_R)\ . \tag{13}$$

The spatial transform matrix for ΣΔ-DDL based hybrid approach is then represented as

$$\mathbf{G}_{\Sigma\Delta} = \begin{bmatrix} \mathbf{w}_{s-\Sigma} & \mathbf{w}_{s-\Delta} \end{bmatrix}. \tag{14}$$

For the ΣΔ-DDL based hybrid approach, the transformation matrix in the temporal domain is given by temporal D^3 weight vectors corresponding to Doppler frequencies f_{-1}, f_0, f_1, in LPR (η_d = 3 Doppler bins)

$$\mathbf{F}_{DDL} = \begin{bmatrix} \mathbf{w}_t(f_{-1}) & \mathbf{w}_t(f_0) & \mathbf{w}_t(f_1) \end{bmatrix}, \tag{15}$$

where $\mathbf{w}_t(f)$ denotes the temporal D^3 weight vector for a Doppler frequency f. Note that this is equivalent to the scheme to set up the temporal transformation matrix in the JDL based hybrid process [11].

Using the spatial and temporal transformation matrices defined above, the overall transformation matrix for the ΣΔ-DDL based hybrid STAP is given by

$$\mathbf{T}_{\Sigma\Delta-DDL} = \mathbf{F}_{DDL} \otimes \mathbf{G}_{\Sigma\Delta}\,. \tag{16}$$

The space-time domain data are transformed to the LPR in the angle-Doppler domain using the transformation matrix $\mathbf{T}_{\Sigma\Delta\text{-}DDL}$, as $\tilde{\mathbf{x}} = \mathbf{T}_{\Sigma\Delta-DDL}^H \mathbf{x}$, $\tilde{\mathbf{s}} = \mathbf{T}_{\Sigma\Delta-DDL}^H \mathbf{s}$ and $\tilde{\mathbf{R}} = \mathbf{T}_{\Sigma\Delta-DDL}^H \mathbf{R} \mathbf{T}_{\Sigma\Delta-DDL}$. After domain transformation, a statistical detection algorithm is applied to the LPR data with weight vector $\tilde{\mathbf{w}} = \tilde{\mathbf{R}}^{-1}\tilde{\mathbf{s}}$, and a target in the primary range cell is declared if, for example, the modified sample matrix inversion (MSMI) statistic [16] is above a chosen threshold (η_o)

$$\eta_{MSMI} = \frac{\left|\tilde{\mathbf{w}}^H \tilde{\mathbf{x}}\right|^2}{\tilde{\mathbf{s}}^H \tilde{\mathbf{R}}^{-1} \tilde{\mathbf{s}}} \underset{H_0}{\overset{H_1}{\gtrless}} \eta_0\ . \tag{17}$$

The MSMI statistic is used in our simulation because it is known be a constant false alarm rate (CFAR) statistic in Gaussian interference.

3.2 ΣΔ- ΣΔ based hybrid algorithm

In the ΣΔ-ΣΔ based hybrid STAP, we further reduce the temporal DOF to two Doppler bins (f_s, f_d; η_d = 2) applying the ΣΔ strategy, using sum and difference temporal beams, instead of the DDL scheme of (15). Let $f_L = f_t - f_{del}$, $f_R = f_t + f_{del}$ be the left and right Doppler frequency with respect to the look Doppler frequency f_t where f_{del} is a properly chosen frequency interval. Similar to the spatial case, sum and difference temporal vectors can be defined as

$$\mathbf{s}_t(f_t) = \{\mathbf{b}(f_L) + \mathbf{b}(f_R)\}, \qquad \mathbf{d}_t(f_t) = \{\mathbf{b}(f_L) - \mathbf{b}(f_R)\}, \tag{18}$$

where $\mathbf{b}(f)$ is the temporal steering vector for look Doppler f.

Based on this fact, the temporal D^3 weights for ΣΔ-ΣΔ based hybrid STAP can be easily obtained in a manner similar to that in equation (13) and (14),

$$\mathbf{w}_{t-\Sigma} = \mathbf{w}_t(f_L) + \mathbf{w}_t(f_R), \quad \mathbf{w}_{t-\Delta} = \mathbf{w}_t(f_L) - \mathbf{w}_t(f_R)\ . \tag{19}$$

The temporal transformation matrix is then

$$\mathbf{F}_{\Sigma\Delta} = \left[\mathbf{w}_{t-\Sigma} \qquad \mathbf{w}_{t-\Delta}\right]. \tag{20}$$

Using the beamformer matrix $\mathbf{G}_{\Sigma\Delta}$ in equation (14) and temporal transformation matrix defined above, the space-time matrix to form the 2×2 LPR for ΣΔ-ΣΔ based hybrid STAP is

$$\mathbf{T}_{\Sigma\Delta-\Sigma\Delta} = \mathbf{F}_{\Sigma\Delta} \otimes \mathbf{G}_{\Sigma\Delta}. \tag{21}$$

As before, the transformation matrix $\mathbf{T}_{\Sigma\Delta-\Sigma\Delta}$ is used to transform both the data and the steering vector as $\widetilde{\mathbf{x}} = \mathbf{T}^{H}_{\Sigma\Delta-\Sigma\Delta}\mathbf{x}$, $\widetilde{\mathbf{s}} = \mathbf{T}^{H}_{\Sigma\Delta-\Sigma\Delta}\mathbf{s}$, $\widetilde{\mathbf{R}} = \mathbf{T}^{H}_{\Sigma\Delta-\Sigma\Delta}\mathbf{R}\mathbf{T}_{\Sigma\Delta-\Sigma\Delta}$, and $\widetilde{\mathbf{w}} = \widetilde{\mathbf{R}}^{-1}\widetilde{\mathbf{s}}$.

The ΣΔ-ΣΔ based hybrid algorithm is the most efficient algorithm considered in this paper, because it uses only 2 spatial channels and 2 temporal DOF.

One potential issue in the use of the ΣΔ algorithm is that of clutter dimensionality. The JDL algorithm provides the flexibility to increase the adaptive DOF to cope with higher dimensional clutter. However, it is worth emphasizing that, in practical non-homogeneous scenarios, the adaptive DOF allowed is determined largely by the training samples available more than the dimensionality of the clutter. In this regard, minimizing the adaptive DOF in the ΣΔ is almost always a positive. The gains are both in the quality of the estimate of the interference covariance matrix and in the reduced computation load. Finally, we conclude this section by noting that there has been little theoretical analysis of the hybrid approaches. Attempts of theoretical analyses have proven to be intractable.

3.3 Comparison of computation load

The algorithms we have discussed so far share a common theme of reduced DOF, and the resulting reduced secondary data. In Table 1 we compare the strategies of reducing DOF and the computation load for different algorithms assuming $M \geq N$. In keeping with the contributions of this paper, the table focuses on the JDL based hybrid, ΣΔ-DDL based hybrid and ΣΔ-ΣΔ based hybrid algorithms.

Table 1: Comparison of hybrid algorithms

	JDL based hybrid	ΣΔ-DDL based hybrid	ΣΔ-ΣΔ based hybrid
Spatial DOF reduction strategy	JDL	ΣΔ	ΣΔ
Temporal DOF reduction strategy	DDL	DDL	ΣΔ
LPR($\eta_a \times \eta_d$)	$\eta_a \times \eta_d$	$2 \times \eta_d$	2×2
Computation load	$L \times \mathbf{O}(((M\text{-}1)(M\text{-}1))^3)$ $\times \eta_a \eta_d \times \mathbf{O}((\eta_a \eta_d)^3)$	$L \times \mathbf{O}(((M\text{-}1)(M\text{-}1))^3)$ $\times 2\eta_d \times \mathbf{O}((2\eta_d)^3)$	$L \times \mathbf{O}(((M\text{-}1)(M\text{-}1))^3)$ $\times 2 \times 2 \times 1/6 \times 4^3$

As is clear from Table 1, reducing the DOF has significant impact on the computation load for the hybrid approach. The smaller the overall DOF becomes, the lower the complexity of the algorithm will be. Considering that a major drawback of the hybrid schemes is their computation load, the development of the ΣΔ-ΣΔ based hybrid algorithm has a significant advantage over previously available hybrid approaches.

3.4 Non-homogeneity detector combined algorithm

A non-homogeneity detector (NHD) is used to detect non-homogeneous cells within the measured data in a CPI. We combine the NHD with the proposed STAP algorithm to improve the performance. Figure 3 shows a comprehensive block diagram for this combination. As shown in the figure, the first step is an NHD that classifies

range cells as non-homogeneous or homogeneous. Once range cells are identified as either non-homogeneous or homogeneous by the NHD, a traditional non-hybrid algorithm is applied for homogeneous cells and a hybrid algorithm for non-homogeneous cells. In both cases, the secondary data required to estimate the interference covariance matrix are obtained using nearby homogeneous range cells.

It should be noted that there are several NHD schemes for clutter model and the choice of an NHD is another topic of STAP research. The NHD chosen in this paper is simply the original statistical STAP applied to the data with no regard for the non-homogeneous characteristics of clutter environment. Range cells with its MSMI statistic above a threshold are treated as non-homogeneous.

4 Simulation results

In this section, we present simulations results to demonstrate performance of the proposed algorithms. The system parameters that are to be used commonly throughout simulations are listed in Table 2. The overall interference is a sum of clutter, barrage noise jamming and discrete interfering sources. The discrete clutter model of Ward [4] is used and the jammer is modelled to be homogeneous in range, arriving from a single angle, but covering all Doppler bins. The discrete interference is a target-like signal, localized in space and Doppler frequency. The jammer, clutter and discrete interferer powers are referenced to the noise level.

Table 2: System parameters

Parameter	Value	Parameter	Value
N, Number of antennas	18	*M*, Number of pulses/CPI	18
Operating frequency	450MHz	PRF	300Hz
Pulse width	200 us	Antenna spacing	half of the wavelength
Look angle (azimuth)	0deg	Look Doppler	100Hz
Instantaneous bandwidth	4MHz	System loss	4dB
Ground reflectivity	-3dB	Element pattern	Cosine
Backlobe attenuation	30dB	Number of clutter patches	361
Clutter range	130km	Transmit array tapering	Uniform
Intrinsic velocity	0 m/s	Platform altitude	9km
Thermal noise power	Unity	Platform velocity	50 m/s
Transmit peak power	400 kW	Velocity misalignment angle	0 deg
β (clutter slope)	1		

4.1 Performance of direct data domain (D^3) algorithm

Performance of the proposed D^3 algorithm which uses the SINR maximization strategy and employs additional three DOF reductions is illustrated in Figure 4. Parameters of the signals such as clutter, jammer and discrete interferers are shown in Table 3. Among the two discrete interferers, only one is used at a time.

Figure 4(A)-(D) shows the adapted patterns resulting from the proposed D^3 algorithm. The beam pattern presented are the mean over 200 trials. The angle plot in Fig. 4(A) clearly shows distinct nulls in the directions of discrete interferer 1 at -33° and the jammer at 20°, while maintaining the array gain to the 0° look direction. Figure 4(B) plots the temporal beam pattern which has nulls near the 0 Hz Doppler of the main beam clutter and

-100 Hz Doppler of interferer 2. Figure 4(C) shows the spatial beam patterns associated with the sum/difference beams used to form the LPR in angle-Doppler domain for ΣΔ-based hybrid algorithms. To form sum/difference beams, left and right beams with angle interval $\phi_{del} = 2\pi/(12N)$ are used. Both beam patterns have nulls in the directions of discrete interferer 1 at -33 ^{o} and the jammer at 20 ^{o}, which illustrate the benefits of using the D^3 weights for the first stage. Similar to the Figure 4(C), Figure 4(D) illustrates the temporal beam patterns for sum/difference beams which have nulls in the Dopplers of main clutter and interferer 2. To form the ΣΔ Doppler beams, $f_{del} = \mathrm{PRF}/(12M)$ is used to derive the left and right weight vectors. These weights suppress discrete interference, transforming the data to the angle-Doppler domain at the same time.

Table 3: Signal parameters for D^3 algorithm

Parameter	Clutter	Jammer	Discrete interferer1	Discrete interferer 2
Power (dB)	30	37	30	35
Angle (degree)	-	20	-33	0
Doppler frequency (Hz)	-	-	100	-100

4.2 Performance of D^3 algorithm under calibration error

Figure 4(E) illustrates the receiver operating characteristic (ROC) curves of the D^3 method when the complex gains of receiver chains are not exactly known. Each antenna is assumed to have a phase error drawn from a uniform distribution in the $[-\pi/8, \pi/8]$ interval, and an amplitude error drawn from a uniform distribution in the $[0, 2]$ interval. For the projection method, eight leading eigenvectors are used to form the signal subspace. As shown in Table 4, one target and one interferer are injected in jammer-free clutter environment. We can see from Figure 4(E) that the target signal cancellation caused by calibration error degrades the detection performance while the projection method gives meaningful performance improvement.

Table 4: Signal parameters for D^3 under calibration error

Parameter	Clutter	Target	Discrete interferer
Power (dB)	30	25	20
Angle (degree)	-	0	-13
Doppler frequency (Hz)	-	100	100

4.3 Performance of the hybrid algorithms

To verify the performance of the hybrid algorithms in non-homogeneous environment, strong artificial target-like signals, which are neither at the look angle nor at the look Doppler, are introduced in clutter of 20dB average power. Three different cases are tested at different range cells. In the first case, a strong target-like interferer is injected in the 30th range cell where no target is presented. This case will test the capability to suppress the discrete interferer. In the second case, a strong target is added in the 50th range cell where an artificial interferer is also present. This case will illustrate the ability to detect a strong target even in the presence of a strong discrete interferer. In the last case, a weak target is injected in the 80th range cell to test the detection performance. Clutter only environment in Table 5 is assumed, and the system parameters are as given in Table 2.

Figure 5(A) depicts the results of the ΣΔ-DDL based algorithms. Here, two angle bins (η_a = 2) and three Doppler bins (η_d = 3) are used to form the LPR, and 24 secondary data vectors to estimate the 6×6 interference covariance matrix. In Figure 5(A), we compare the MSMI output of the ΣΔ-DDL STAP with that of the ΣΔ-DDL based hybrid algorithm. In the 30th range cell, the hybrid algorithm suppresses the non-homogeneity in the first D^3 stage while the ordinary ΣΔ-DDL algorithm detects the interferer as a strong target. The 50th range bin

represents the second case where a strong target is also present. Note that the hybrid algorithm detects the target not affected by the D^3 stage that suppresses the interferer in the same cell. The last case of the 80th range cell shows that the weak target can be detected by both hybrid and ordinary ΣΔ-DDL algorithm.

Table 5: Signal parameters for hybrid algorithms

Parameter	Clutter	Discrete interferer 1	Discrete interferer 2	Strong target	Weak target
Power (dB)	20	20	25	10	0
Angle (degree)	-	0	-33	0	0
Doppler frequency (Hz)	-	120	100	100	100
Range cell	-	30	50	50	80

As shown in Figure 5(B), the ΣΔ-ΣΔ based hybrid algorithm produces similar results to ΣΔ-DDL based hybrid case with smaller DOF and fewer secondary data vectors. We use two angle bins ($\eta_a = 2$) and two Doppler bins ($\eta_d = 2$) for LPR and 16 secondary range cells to estimate the interference covariance matrix. The corresponding figure illustrates the ability of the simple ΣΔ based algorithms to provide effective interference suppression and target detection. Note that the ΣΔ based schemes require fewer secondary range cells than with the JDL based hybrid approach in [11].

4.4 Effect of the non homogeneous detector (NHD)

To test the performance of the hybrid algorithms combined with the NHD in Section 3.4 in a non-homogeneous environment, the non-Gaussian SIRV clutter model [5-7] is used. Since jammers can be suppressed prior to the signal processing a clutter-only environment with 20dB average CNR is assumed. See Table 6.

Table 6: Signal parameters for the combined algorithms

Parameter	Clutter	Discrete interferer 1	Discrete interferer 2	Strong target	Weak target
Power (dB)	20	35	30	12	0
Angle (degree)	-	-33	0	0	0
Doppler frequency (Hz)	-	100	120	100	100
Range cell	-	20	80	50	44

To make the environment even more heterogeneous, artificial target-like interferers are introduced. Discrete interferer 1 is in the 20th range cell, with 35dB power at -33^o angle. Discrete interferer 2 is in the 80th range cell with 30dB power and 120 Hz Doppler. A target is injected in the 50th range cell with 12 dB SNR and another in the 44th range cells with 0 dB SNR. Since the two targets are located close, one will be included in the other's secondary data set when the interference statistics is estimated.

Figure 6 presents the performance of the combined-STAP that uses ΣΔ-DDL based hybrid algorithm while Figure 7 represents that of the combined-STAP using ΣΔ-ΣΔ based hybrid algorithm. Figure 6(A) shows the MSMI statistics of (17) for the ordinary ΣΔ-DDL algorithm, which erroneously declares the discrete interferers in the 20th and 80th ranges cells as strong targets. This result clearly calls for the hybrid algorithm that identifies and eliminates non-homogeneities in the secondary data. Also note that the weak target in the 44th range cell is obscured because of the strong target in the secondary data.

Figure 6(B) illustrates benefits of the NHD in non-homogeneous environments. Here the ΣΔ-DDL based NHD first identifies the range cells with strong response as non-homogeneous cells, and removes them from secondary data. Those removed cells may contain a strong target or a strong discrete interferer, and this removal allows the weak target in the 44th cell to be detected. However, the ΣΔ-DDL only algorithm which cannot be informed about discrete non-homogeneity within the primary range cell is not able to suppress discrete interferers

in the 20th and 80th range cells despite the use of NHD. On the other hand, the combined-STAP algorithm of Figure 3 that employs the hybrid algorithm for non-homogeneous range cells can detect both strong and weak targets while suppressing discrete interferers. The result is illustrated in Figure 6(C).

The performance of the combined-STAP using the ΣΔ-ΣΔ based hybrid algorithm is comparable to that of the ΣΔ-DDL based hybrid, however, at significantly lower computation cost of 4 instead of 6 D^3 solutions. Figure 7 illustrates the results of this efficient algorithm.

4.5 Receiver operating characteristic (ROC) curves

Figure 8(A) presents the ROC curves of the ΣΔ-DDL based algorithms in non-homogeneous clutter environment while Figure 8(B) represents those of ΣΔ-ΣΔ based approaches. The resultant curves are obtained using 5000 Monte Carlo simulations. In this simulation, four approaches are compared, the ordinary statistical algorithm, the ordinary statistical algorithm with selected homogeneous trainings by NHD, the D^3 method and the combined-hybrid algorithm.

For the case of the ΣΔ-DDL based algorithm, an artificial interferer which has 25dB power and 20Hz offset from the look Doppler and a target with 10dB SNR are introduced to the test cell in the 20dB CNR clutter environment. These parameters are summarized in Table 7.

Table 7: Signal parameters for ΣΔ-DDL based algorithms

Parameter	Clutter	Target	Discrete interferer
Power (dB)	20	10	25
Angle (degree)	-	0	0
Doppler frequency (Hz)	-	100	120

The result of two statistical algorithms illustrates the benefits of the NHD. Secondary sample support of the purely statistical approach is not as homogenous as that of the method using NHD. Inaccurate covariance matrix estimation by inappropriate trainings contributes to a higher false alarm rate or a lower target detection probability. However, the ΣΔ-DDL algorithm which cannot be informed about discrete non-homogeneity within the primary range cell is not able to deal with the discrete non-homogeneity. Therefore, in the severe non homogeneous environment, the D^3 algorithm achieves a better performance than the ordinary statistical algorithm regardless of the NHD presence. Finally, the combined-hybrid STAP that employs the ΣΔ-DDL based hybrid algorithm for non-homogeneous cells and ΣΔ-DDL method for homogeneous cells shows the best curve. This result gives the justification of each part of the final combined algorithm which makes it practical in the real world.

Figure 8(B) illustrates the comparable results of the more efficient ΣΔ-ΣΔ based algorithms. In this case, an interferer with 20dB power and 20Hz offset from the look Doppler and a target with 12dB SNR is injected to the test cell in the 10dB CNR environment as shown in Table 8.

Table 8: Signal parameters for ΣΔ- ΣΔ based algorithms

Parameter	Clutter	Target	Discrete interferer
Power (dB)	10	12	20
Angle (degree)	-	0	0
Doppler frequency (Hz)	-	100	120

5 Conclusions

In this paper, we present various improvements of the available JDL based hybrid algorithm designed for non-homogeneous clutter. We first formulate a stable version of the D^3 STAP algorithm of [11, 13]. The modified D^3 algorithm is reliable since it does not require an emphasis parameter. Furthermore, the new D^3 algorithm is made to be more stable by employing the forward smoothing technique in [26]. However, a major contribution would be the development of a lower complexity hybrid algorithm based on the efficient ΣΔ algorithm in [8]. The hybrid algorithm uses the new modified D^3 algorithm as an underlying adaptive transformer to the angle-Doppler domain. Here we present two versions of hybrid processing based on the ΣΔ-DDL STAP and the ΣΔ-ΣΔ STAP. The ΣΔ based hybrid algorithm has significantly lower computation load, alleviating one of the key drawbacks of the original hybrid algorithm. Finally, the ΣΔ based hybrid STAP is placed here within the framework of knowledge-based STAP processing. The combined-STAP formulation uses a NHD to identify non-homogeneous range cells. It should be noted that there are several NHD schemes for the SIRV clutter model with good performance leaving open the possibility of even better performance in non-homogeneous environments.

Acknowledgement

This research was supported by the Agency for Defence Development, Korea, through a radar signal processing contract.

References

[1] G.H. Golub and C.F. Van Loan, “Matrix Computation”, Johns Hopkins University Press, 1996

[2] H. Wang and L. Cai, “On adaptive spatial-temporal processing for airborne surveillance radar systems”, *IEEE Trans. on Aerospace and Electronic Systems*, v. 30,NO.3, pp. 660-669,July 1994.

[3] I. Reed, J. Mallett, and L. Brennan, Rapid convergence rate in adaptive arrays," *IEEE Trans. on Aerospace and Electronic Systems*, v. AES-10, pp. 853-863, 1974.

[4] J. Ward, “Space-time adaptive processing for airborne radar", Tech. Rep. F19628-95-C-0002, MIT Lincoln Laboratory, December 1994.

[5] M. Rangaswamy, D. Weiner, A. Ozturk, “Non-Gaussian random vector identification using Spherically Invariant Random Processes”, *IEEE Transactions on Aerospace and Electronic Systems*, V.29, No.1, January 1993

[6] M. Rangaswamy, D. Weiner, A. Ozturk, “Computer Generation of Correlated Non-Gaussian Radar Clutter”, *IEEE Transactions on Aerospace and Electronic Systems*, V.31, No.1, January 1995

[7] M. Rangaswamy, “Statistical Analysis of the non-homogeneity detector for Non-Gaussian Interference Backgrounds”, *IEEE Transactions on Signal Processing*, V.53, No.6, June 2005

[8] R.D. Brown, R.A. Schneible, M.C. Wicks, H.Wang and Y.Zhang, “STAP for clutter suppression with Sum and Difference Beams”, *IEEE Transactions on Aerospace and Electronic Systems* v. 36, No.2. April 2000

[9] R. DiPietro, ”Extended factored space-time processing for airborne radar systems,” *Proceedings of the 26th Asilomar Conference on Signals, Systems, and Computing, Pacific Grove, CA,* October, 1992, pp425-430

[10] R.S. Adve, T.B. Hale, and M.C. Wicks, ”Practical joint domain localised adaptive processing in homogeneous and non-homogeneous environments Part I: Homogeneous Environments", *IEE Proc.Radar. Sonar Navig*., v.147, no.2, pp.57-65, April. 2000.

[11] R.S. Adve, T.B. Hale, and M.C. Wicks, ”Practical joint domain localised adaptive processing in homogeneous and non-homogeneous environments Part II:Non-homogeneous environments", *IEE Proc. Radar. Sonar Navig.*, v.147, no.2, pp.66-73, April. 2000.

[12] R.S. Adve, M.C. Wicks, T.B. Hale, P. Antonik, “Ground moving target indication using knowledge based space-time adaptive processing”, *2000 IEEE International Radar Conference*, Washington DC, May 2000.

[13] T.K. Sarkar and N. Sangruji, “An adaptive nulling system for a narrow-band signal with a look-direction constraint utilizing the conjugate gradient method”, *IEEE Transactions on Antennas and Propagation*, v. 37, No.7, July 1989.

[14] W. Koch and R. Klemm, “Ground target tracking with STAP radar”, *IEE Proc.-Radar. Sonar Navig.,* v.148, no.3, June. 2001.

[15] W.L. Melvin, “A STAP Overview", *IEEE Aerospace and Electronic Systems Magazine*, v.19, No.1, Jan.2004

[16] Chen. W.,and Reed,I.S., “ A new CFAR detection test for radar”, *Digital Signal Processing*, v.1, No.4, Oct.1991

[17] R.S. Adve and T.K. Sarkar, “Compensation of the effects of mutual coupling on direct data domain algorithms”, *IEEE Trans. on Antennas and Propagation*, vol. 48, no. 1, pp. 86-94, January 2000.

[18] H.W. Engl, M. Hanke and A. Neubauer, “Regularization of Inverse Problems”, Kluwer Academic Publishers, 1996

[19] M.C. Wicks, M. Rangaswamy, R.S. Adve and T.B. Hale, “Space-time adaptive processing: A knowledge based perspective”, *IEEE Signal Processing Magazine*, vol. 23, no. 1, pp. 51-65, January 2006.

[20] M. Rangaswamy, F. Lin, and K. Gerlach, “Robust adaptive signal processing methods for heterogeneous radar clutter scenarios”, *Signal Processing*, vol. 84, pp. 1653–1665, 2004.

[21] M.C. Wicks, W.L. Melvin, and P. Chen, “An efficient architecture for nonhomogeneity detection in space-time adaptive processing airborne early warning radar”, *Proceedings of the 1997 International Radar Conference*, October 1997. Edinburgh, UK.

[22] W. L. Melvin and M.C. Wicks, “Improving practical space-time adaptive radar” *Proceedings of the 1997 IEEE National Radar Conference*, May 1997

[23] J.F.Bull, M.A. Arnao, and L. R. Burgess, “Hypersensitivity effects in adaptive antenna arrays,” *IEEE Antenna Propagat.SoC.Symp*., May 1990, pp. 396-399

[24] David D. Feldman, Lloyd J. “A Projection Approach for Robust Adaptive Beamforming”, *IEEE Transactions on signal processing,*vol.42, No.4, April 1994

[25] MATHER, J., REES, H.D., and SKIDMORE, I.D. “Adaptive clutter and jammer cancellation for element digitised airborne radar”, Proceedings of the ASILOMAR 99 Conference\

[26] Pillai, S. U., Kim, Y.L. and Guerci,J.R.: “Generalized forward/backward subaperture smoothing techniques for sample starved STAP”, IEEE Tranas. On Signal Processing, 2000,48,(12), pp. 3569-3574

[27] M. Wax and T. Kailath, “Detection of signals by information theoretic criteria,” IEEE Transactions on Acoustics, Speech, and Signal Processing, vol. 33, no. 2, pp. 387–392, Apr. 1985.

6. Figures

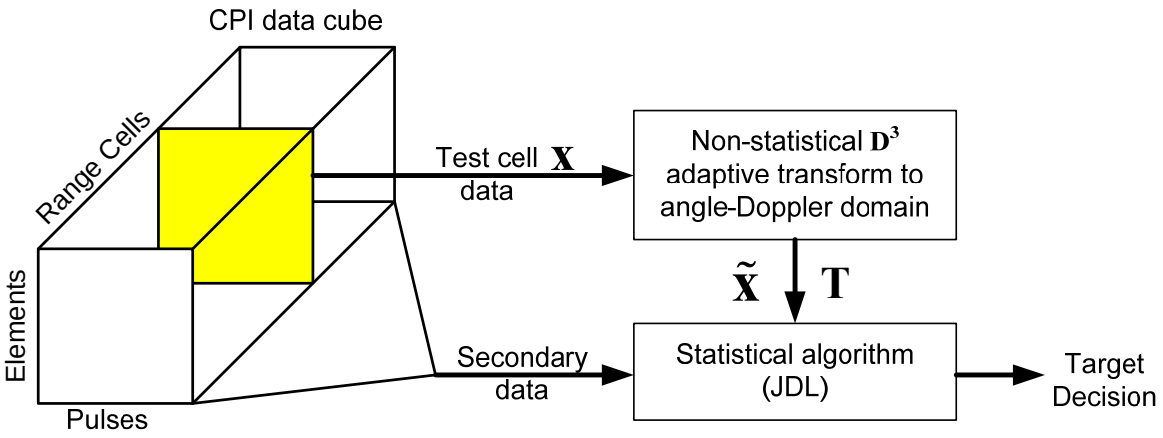

Figure 1: Block diagram of the two-stage JDL-based hybrid algorithm

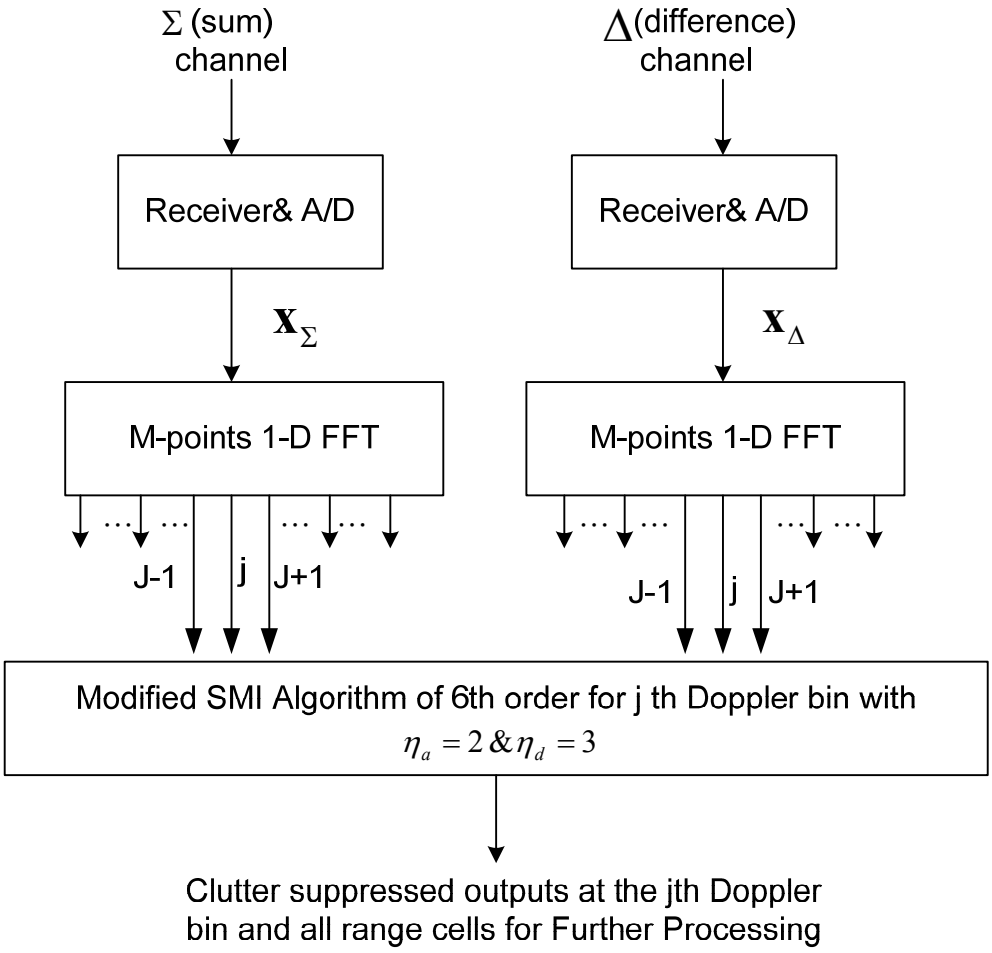

Figure 2: Block diagram of the ordinary ΣΔ-DDL STAP

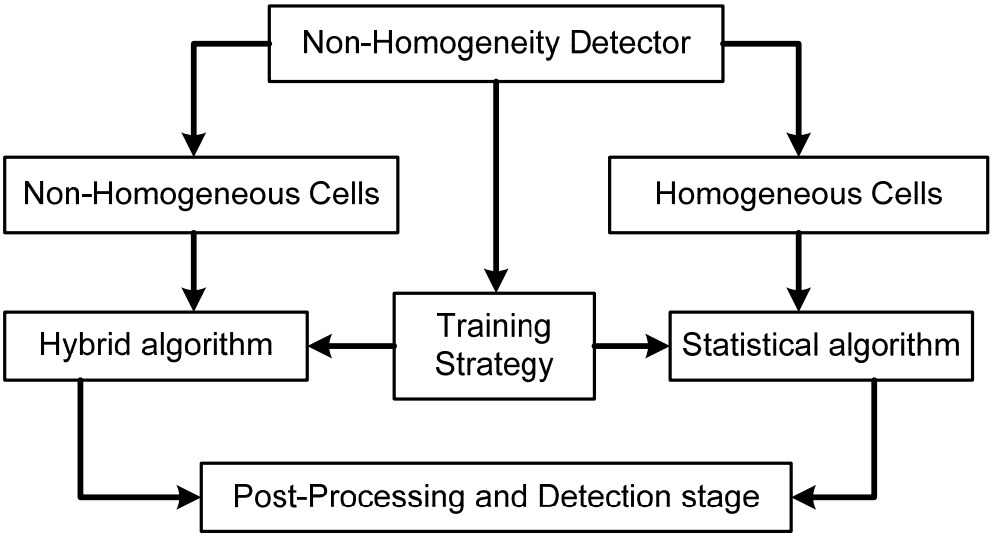

Figure 3: Block diagram of the combined space-time adaptive processing (combined-STAP)

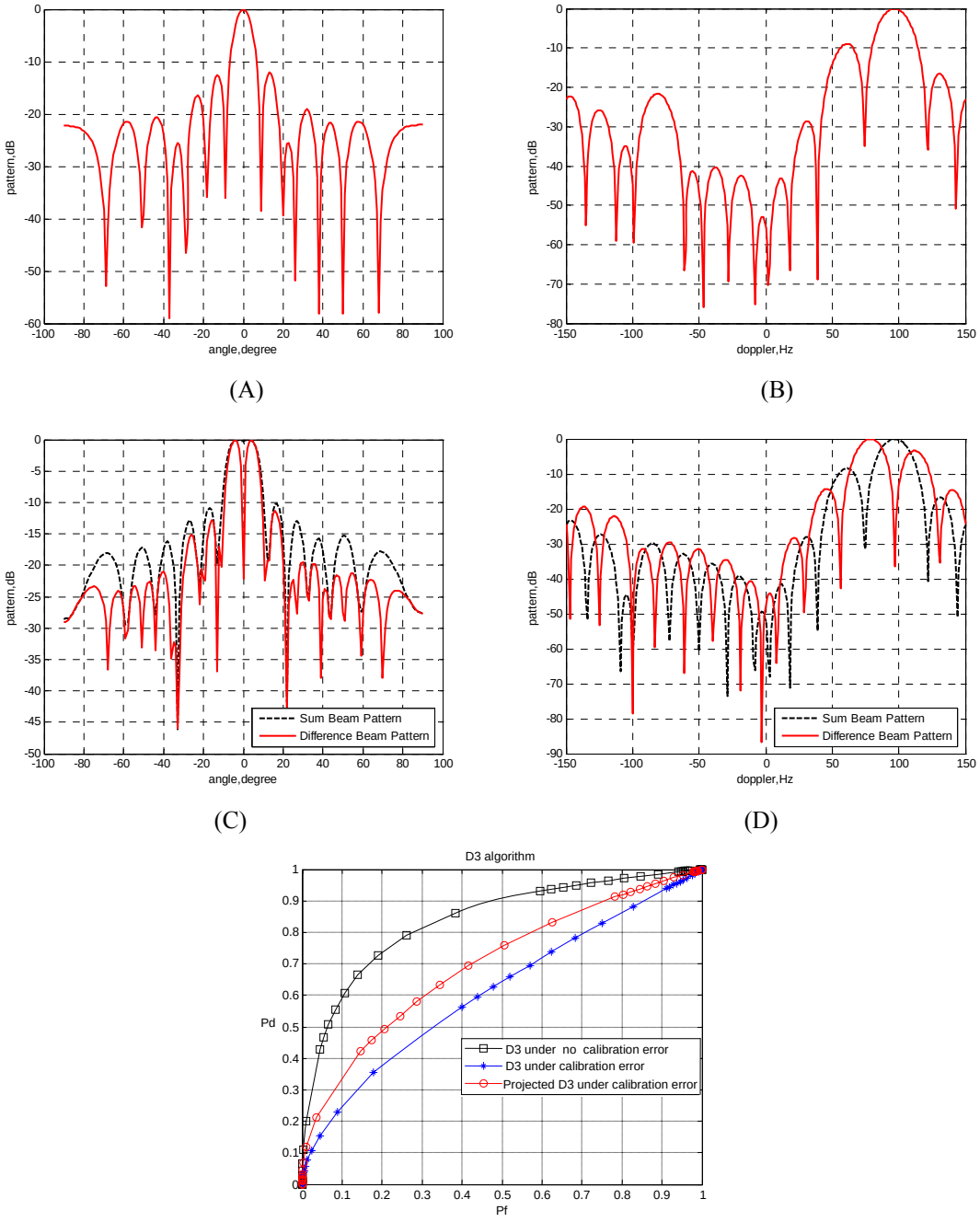

Figure 4: Performance of the modified D^3 algorithm using the SINR maximization

(A) Adapted spatial pattern for the 0 ^{o} look direction with nulls in the directions of the discrete interferer at -33 ^{o} and of the jammer at 20 ^{o}. (B) Adapted Doppler pattern for the 100Hz look doppler with nulls near the 0 Hz Doppler of main beam clutter and at the -100 Hz interferer. (C) Sum/difference D^3 spatial patterns for the 0 ^{o} look direction with nulls at the -33 ^{o} discrete interferer and at the 20 ^{o} jammer. (D) Sum/difference D^3 temporal patterns for the 100Hz look Doppler with nulls near the 0 Hz Doppler of the main beam clutter and at the -100 Hz interferer. (E) ROC curves under calibration errors.

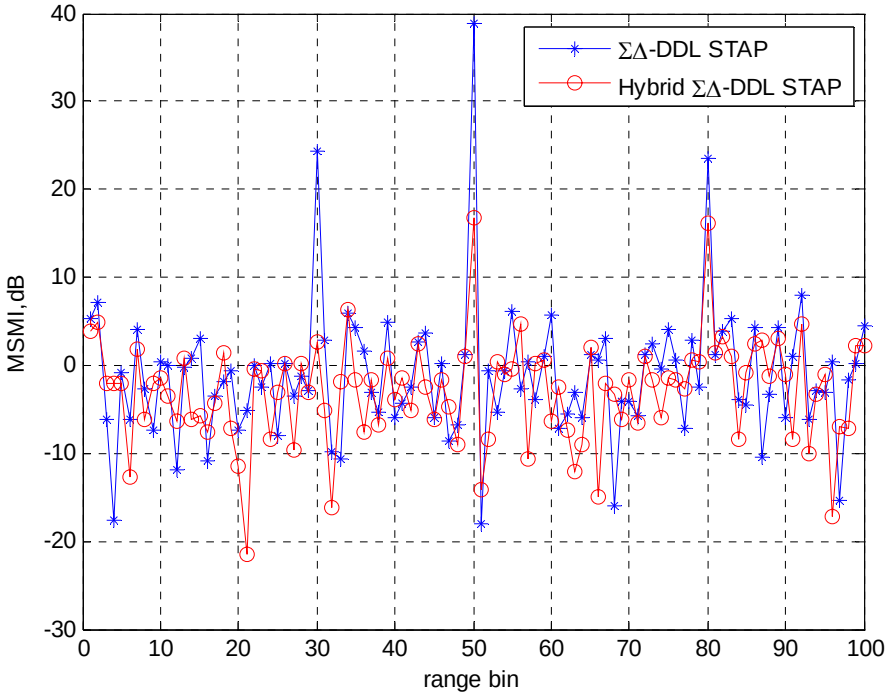

(A)

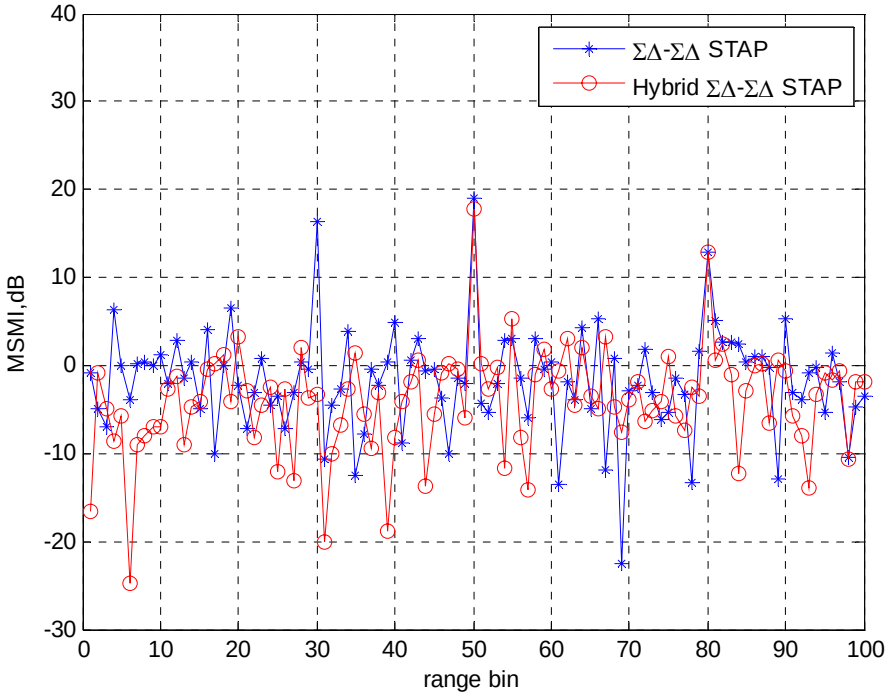

(B)

Figure 5: Performance of hybrid algorithms in countering non-homogeneities. The 30th range cell contains a strong interferer, the 50th range cell has a strong interferer and a strong target, and the 80th range cell has a weak target.

(A) ΣΔ-DDL based algorithms. (B) ΣΔ- ΣΔ based algorithms

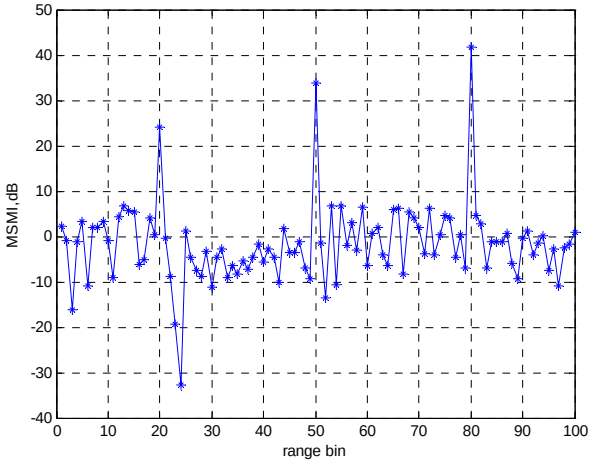

(A)

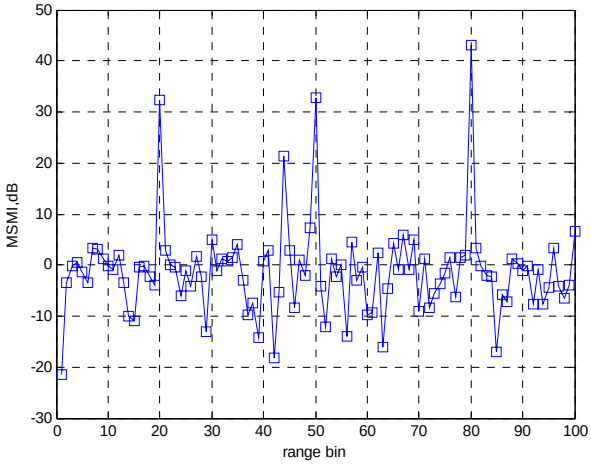

(B)

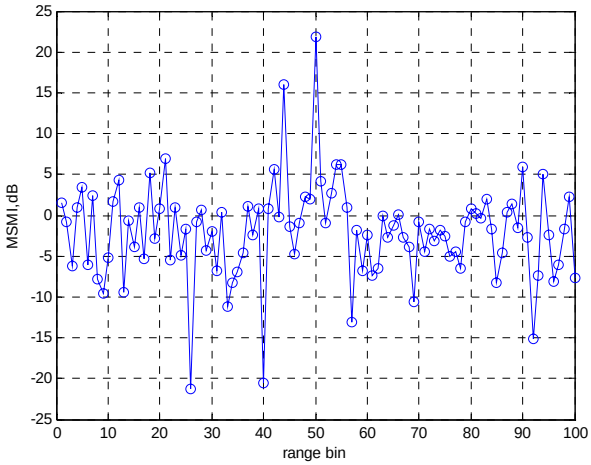

(C)

Figure 6: Performance of the ΣΔ-DDL based hybrid algorithm for target detection in non-homogeneous environment. The 20th and 80th range cells contain strong interferers, the 44th range cell contains a weak target, and the 50th range cell contains a strong target.
(A) ΣΔ-DDL only (B) ΣΔ-DDL with NHD (C) Combined-STAP using ΣΔ-DDL based hybrid algorithm.

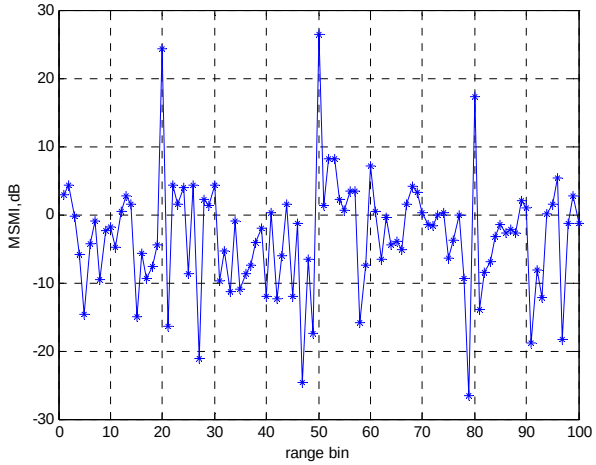

(A)

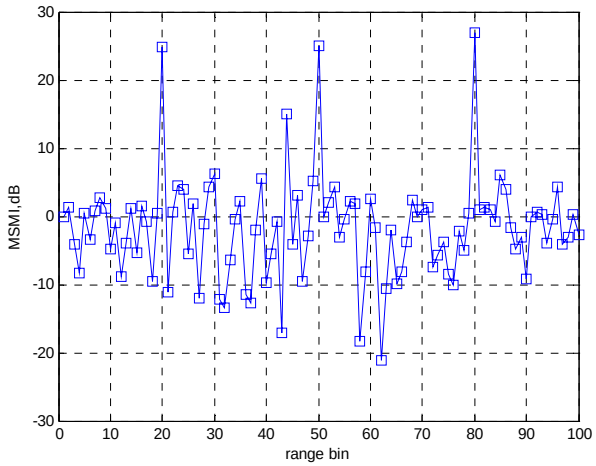

(B)

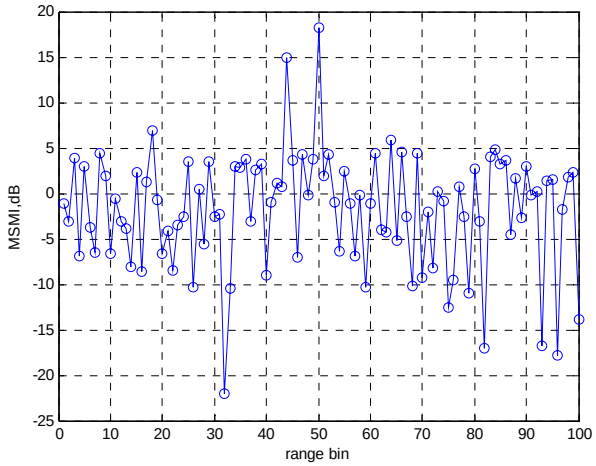

(C)

Figure 7: Performance of the ΣΔ-ΣΔ based hybrid algorithm for target detection in non-homogeneous environment. The 20th and 80th range cells contain strong interferers, the 44th range cell has a weak target, and the 50th range cell contains a strong target.
(A) ΣΔ- ΣΔ only (B) ΣΔ- ΣΔ with NHD (C) Combined-STAP using ΣΔ-ΣΔ -hybrid algorithm.

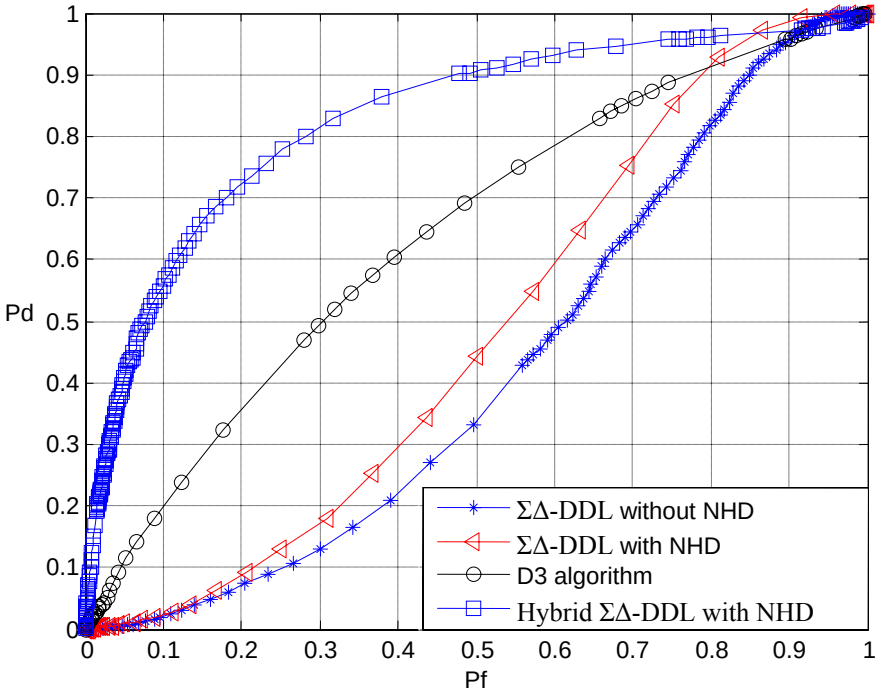

(A)

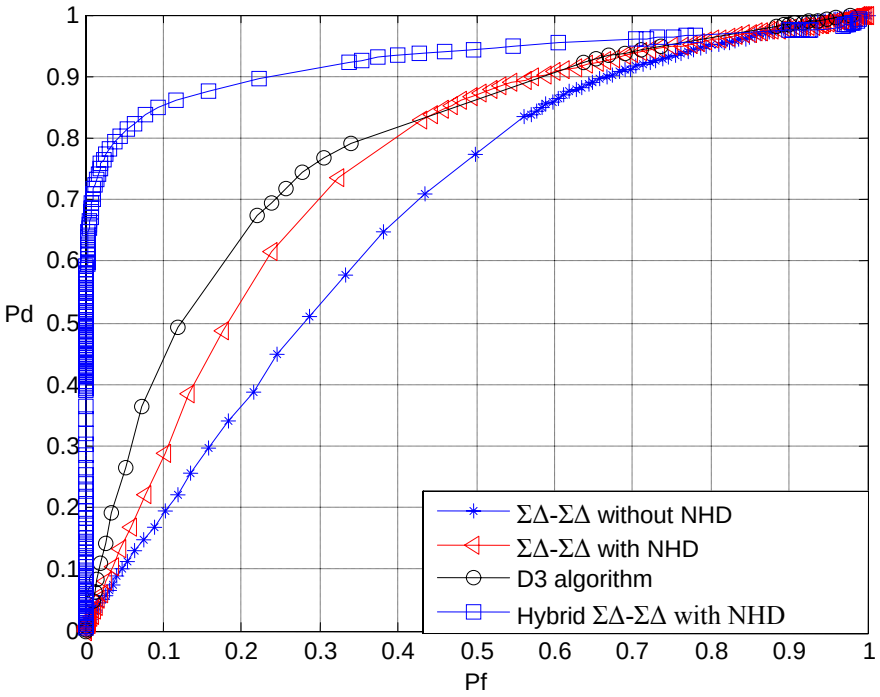

(B)

Figure 8: Performance of the proposed algorithms for target detection in non-homogeneous environment (A) ΣΔ-DDL based algorithms (B) ΣΔ-ΣΔ based algorithms